Critical x-ray scattering studies of Jahn-Teller phase transitions in $TbV_{1-x}As_xO_4$

K. C. Rule,[1] M. J. Lewis,[1] H. A. Dabkowska,[1] D. R. Taylor,[2] and B. D. Gaulin[1,3]
[1]*Department of Physics and Astronomy, McMaster University, Hamilton, Ontario, Canada L8S 4M1*
[2]*Department of Physics, Engineering Physics, and Astronomy, Queen's University, Kingston, Ontario, Canada K7L 3N6*
[3]*Canadian Institute for Advanced Research, 180 Dundas Street W., Toronto, Ontario, Canada M5G 1Z8*
(Received 9 January 2008; revised manuscript received 20 March 2008; published 30 April 2008)

The critical behavior associated with the cooperative Jahn-Teller phase transitions in $TbV_{1-x}As_xO_4$ (where $x=0,0.17,1$) single crystals have been studied by using high-resolution x-ray scattering. These materials undergo continuous tetragonal→orthorhombic structural phase transitions that are driven by the Jahn-Teller physics at $T_C=33.26(2)$, 30.32(2), and 27.30(2) K for $x=0$, 0.17, and 1, respectively. The orthorhombic strain was measured close to the phase transition and was shown to display mean field behavior in all three samples. Pronounced fluctuation effects are manifest in the longitudinal width of the Bragg scattering, which diverges as a power law, with an exponent given by $x=0.45\pm0.04$, on approaching the transition from either above or below. All samples exhibited twinning; however, the disordered $x=0.17$ sample showed a broad distribution of twins that were stable to relatively low temperatures, well below T_C. This indicates that while the orthorhombic strain continues to develop in a conventional mean field manner in the presence of disorder, twin domains are easily pinned by quenched impurities and their associated random strains.

DOI: 10.1103/PhysRevB.77.134116 PACS number(s): 64.70.kp, 75.40.−s, 61.50.Ks

I. INTRODUCTION

$TbVO_4$ and $TbAsO_4$ belong to a group of compounds that undergo a structural phase transition induced by the cooperative Jahn-Teller effect. Both $TbVO_4$ and $TbAsO_4$ exhibit a transition from the tetragonal $I4_1/amd$ structure at high temperatures to the twinned orthorhombic $Fddd$ phase at temperatures below 35 K.[1] At room temperature, the low-lying crystal electric field levels for the Tb^{3+} ions in the $TbVO_4$ environment consist of two singlets separated by 2.23 meV and a degenerate, non-Kramers doublet midway between the singlets.[2,3] The Jahn-Teller phase transition changes the local Tb^{3+} environment, with a concomitant splitting of the doublet and an increase in the singlet separation to 6.32 meV.[3] The resulting magnetic ground state for the Tb^{3+} ions can then magnetically order at much lower temperatures.[4] Structural phase transitions have also been studied in disordered systems wherein the nonmagnetic cations are mixed. Disordered materials such as $TbV_{1-x}As_xO_4$ are characterized by the presence of quenched random strains that are introduced by the ionic radius mismatch between V^{5+} and As^{5+}, which is quite large, being ~20%.

These materials and their Jahn-Teller phase transitions have been known and studied for some time. For example, optical birefringence studies of the critical properties of $TbVO_4$ and $DyVO_4$ showed that the former displayed mean field criticality near its Jahn-Teller transition, while the latter displayed three-dimensional (3D) Ising-type universality near its transition.[5] Early x-ray experiments measured the order parameter relevant to these Jahn-Teller transitions, which is the orthorhombic strain, but were not able to give accurate critical property measurements for this family of terbium oxides.[6,7] An x-ray scattering study of the related $TbV_{1-x}P_xO_4$ system[8] has been carried out, although, again, the emphasis was not on the critical regime.

The role of quenched disorder on the Jahn-Teller phase transitions in the $TbV_{1-x}As_xO_4$ system has more recently been the subject of further optical birefringence studies, which also show changes in criticality that are induced by the presence of impurities.[9] The change in criticality has been discussed in the context of the random-field Ising model[10] and how it may be realized in a structural analog of the more familiar case arising in magnetism—that of a dilute Ising antiferromagnet in the presence of a uniform magnetic field.[11]

We have carried out a high-resolution x-ray scattering study of the tetragonal to orthorhombic Jahn-Teller phase transitions in the $TbV_{(1-x)}As_xO_4$ system, with particular emphasis on the critical regime, where the orthorhombic strain is small and fluctuations in the strain may be expected to be large. This will enable a quantitative microscopic understanding of the critical phenomena in the pure, end members of the family and show the extent to which the critical behavior in the mixed system is modified by the presence of quenched disorder.

II. EXPERIMENTAL DETAILS

Single crystals of $TbVO_4$ and $TbAsO_4$ and their solid solutions were grown from PbO/PbF_2 flux by the slow cooling method. Preannealed starting materials Tb_2O_3 and X_2O_5 where X is either V or As were weighed and combined with PbO and PbF_2, which act as high temperature solvents. The mixture was then melted in a Pt crucible at 1300 °C and slow cooled (1°–2°/h) to 900 °C.[12,13] Single crystals in the form of elongated rods with typical dimensions of $5\times2\times2$ mm^3 were separated from this melt. The $TbV_{0.83}As_{0.17}O_4$ single crystal studied was the same as the one previously studied by Schriemer *et al.*[14] In that study, the relative As concentration in $TbV_{1-x}As_xO_4$ is given as $x=0.15$, which is in good agreement with the value $x=0.17$, which we have determined from the current x-ray measurements.

X-ray scattering measurements were performed by using a rotating-anode, Cu K_α x-ray source and a four circle diffractometer that employs a two-dimensional area detector. The single crystals were mounted within a helium-filled sample cell that was attached to the cold finger of a closed-cycle helium refrigerator. Scattering measurements were carried out as a function of temperature with a temperature stability of ~0.005 K, which is appropriate for critical scattering studies. Cu $K_{\alpha 1}$ radiation from the 18 kW rotating anode x-ray generator was selected by using a perfect single crystal Ge (110) monochromator. The diffracted beam was measured by using a Bruker HiStar area detector, which was mounted on the scattering arm at a distance of 0.7 m from the sample. This configuration allowed for high-resolution characterization of the Bragg peaks. The scattered intensity was measured as a function of temperature for both the (6, 6, 0) Bragg reflection in the tetragonal phase, which splits into the (12, 0, 0) and (0, 12, 0) reflections in the twinned orthorhombic phase, and the (8, 0, 0) Bragg reflection in the tetragonal phase, which splits into the (8, 8, 0) and (8,−8,0) reflections in the same twinned orthorhombic phase.

III. MEASUREMENTS OF THE ORTHORHOMBIC STRAIN

Figure 1 shows the representative x-ray scattering contour maps taken for $TbVO_4$, $TbAsO_4$, and $TbV_{0.83}As_{0.17}O_4$ above and below their appropriate phase transition temperatures. Figures 1(a) and 1(b) show the data taken around the (8, 8, 0) Bragg position (in the orthorhombic phase) in $TbVO_4$, while Figs. 1(c)–1(h) show the data taken around the (12, 0, 0) Bragg positions (in the orthorhombic phase) in $TbVO_4$, $TbAsO_4$, and $TbV_{0.83}As_{0.17}O_4$, respectively. All of these scattering data sets were acquired by integrating the Bragg scattering in the vertical direction for each sample rotation angle (Ω plotted on the y axis of Fig. 1) and then plotting the resulting intensity as a function of the scattering angle 2θ. The dashed line in Fig. 1(c) indicates a longitudinal scan, while a vertical line on any of these panels would indicate a transverse scan. The transverse splitting of the (8, 0, 0) tetragonal Bragg peak into (8, 8, 0) orthorhombic Bragg peaks in $TbVO_4$ is shown in Figs. 1(a) and 1(b), while the longitudinal splitting of the tetragonal (6, 6, 0) Bragg peaks into twin orthogonal peaks at (12, 0, 0) and (0, 12, 0) in all three Tb-based oxides is seen in Figs. 1(c)–1(h).

These data sets can be analyzed by extracting the positions for all of the Bragg peaks in the field of view in both the scattering angle 2θ and the sample orientation angle Ω. The scattering angle for the single crystal peaks in both the tetragonal phase above T_C and the twinned orthorhombic phase below T_C is used to extract the relevant lattice parameters and orthorhombic strain, which is defined as the difference between the a and b lattice parameters. The scattering angles for all of the (6, 6, 0) (tetragonal phase) and (12, 0, 0) (orthorhombic phase) Bragg peaks of all three samples are shown as a function of temperature in Fig. 2. Figure 3(a) shows the corresponding orthorhombic strain below T_C in all three samples. Figure 3(b) shows the splitting in domain orientation for $TbVO_4$, $TbAsO_4$, and $TbV_{0.83}As_{0.17}O_4$, which was extracted from the difference in sample orientations,

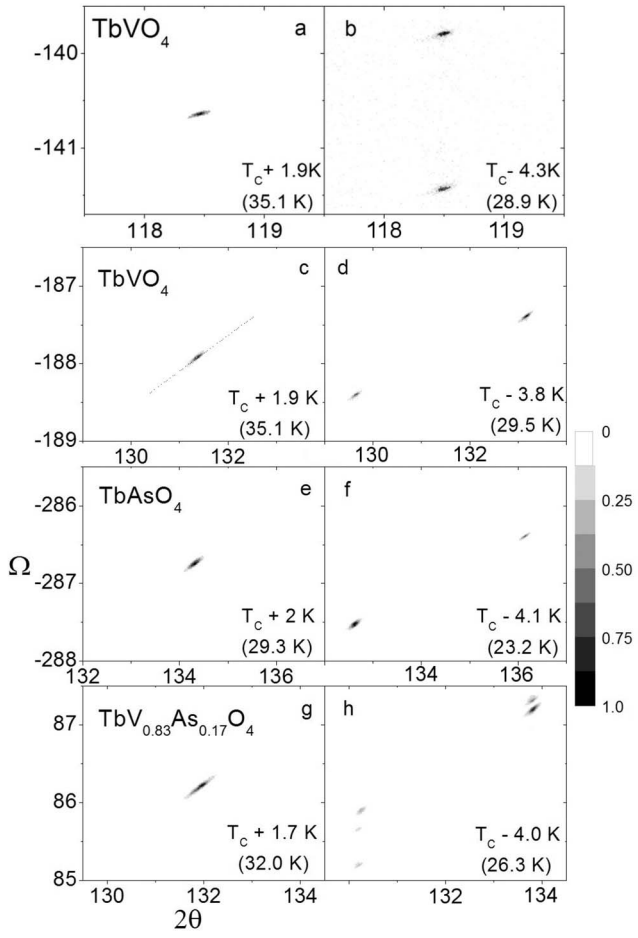

FIG. 1. Representative contour maps of the temperature dependence of the Bragg peaks that split on going through the Jahn-Teller phase transitions in $TbVO_4$, $TbAsO_4$, and $TbV_{0.83}As_{0.17}O_4$. (a) and (b) show the splitting of the (8, 0, 0) Bragg peak into the (8,8,0)/(8,−8,0) Bragg peaks in $TbVO_4$. (c) and (d), (e) and (f), and (g) and (h) show the splitting of the (6, 6, 0) Bragg peak into the (12, 0, 0) and (0, 0, 12) Bragg peaks in $TbVO_4$, $TbAsO_4$, and $TbV_{0.83}As_{0.17}O_4$, respectively. The data on the left [(a), (c), (e), and (g)] are above T_C, while the data on the right [(b), (d), (f), and (h)] are below T_C. The diagonal line in (b) indicates the cut used for the longitudinal scans in Fig. 5. A vertical line would indicate a transverse scan.

which are the Ω positions, of the Bragg peaks from the principal (12, 0, 0) and (0, 12, 0) orthorhombic twin domains below T_C.

Figure 2(a) shows the splitting of the (12, 0, 0) and (0, 12, 0) Bragg peaks in all three systems in absolute units of the scattering angle, while Fig. 2(b) shows the same data, but now relative to the scattering angle of the Bragg peak in the high temperature tetragonal (HTT) phase. These data quite clearly show that all three samples display continuous phase transitions, as was previously known for $TbVO_4$ (Ref. 6) and $TbAsO_4$,[15] and that their critical properties are similar. The scattering in Fig. 2(a), however, also shows that within the high temperature tetragonal phase, the lattice parameter (identified by its scattering angle) for $TbV_{0.83}As_{0.17}O_4$ lies at ~17% of the way between $TbVO_4$ and $TbAsO_4$, as given by a linear variation in lattice parameter between the end mem-

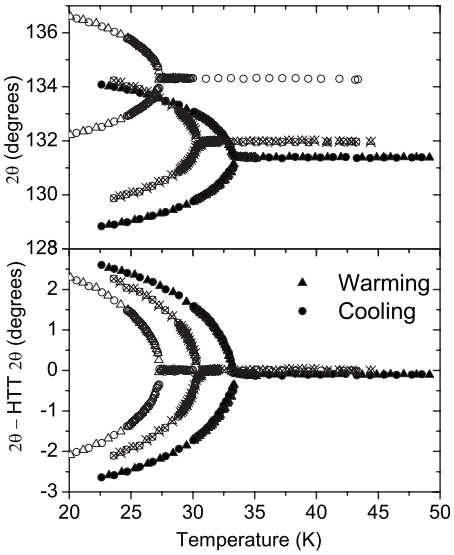

FIG. 2. The temperature dependence of the peak position in 2θ for each of the three samples: $TbVO_4$ (closed symbols), $TbAsO_4$ (open symbols), and $TbV_{0.83}As_{0.17}O_4$ (crossed symbols). The structural phase transition is indicated by the splitting of the single Bragg intensity into two with decreasing temperature. The top panel shows the true 2θ splitting for each of the compounds, while the bottom panel shows the splitting relative to the scattering in the tetragonal phase at high temperatures.

bers of the series, $TbVO_4$ and $TbAsO_4$. Such a linear variation is observed in the $TbV_{1-x}P_xO_4$ system.[8] This establishes an accurate concentration for the $TbV_{0.83}As_{0.17}O_4$ single crystal by microscopic means.

Figure 3(a) shows the corresponding orthorhombic strains, which are defined as the difference in lattice parameters a and b, as a function of temperature below T_C for each of $TbVO_4$, $TbAsO_4$, and $TbV_{0.83}As_{0.17}O_4$. Related measurements of the orthorhombic strain have been previously measured as a function of temperature for the $TbV_{1-x}P_xO_4$ system.[8] However, the present measurements are taken sufficiently close to the phase transitions such that an accurate determination of T_C and a quantitative study of the critical properties of these phase transitions is possible. It is clear from the data that the order parameter, the orthorhombic strain, very sharply rises with decreasing temperature, such that little of this data would reside in the asymptotic critical regime, wherein the order parameter is small compared to its saturation value. Therefore, we fit these data to a full mean field solution,

$$m = \tanh\left[\frac{qJm}{k_BT}\right], \tag{1}$$

rather than simply to the asymptotic expression for small values of the order parameter. This gives a mean field critical exponent for the order parameter, $\beta=0.5$, but the full data sets are accurately described. This description of the order parameters as a function of temperature that uses the solution to transcendental Eq. (1) is shown as the solid lines in Figs. 3(a) and 3(b). Clearly, the full mean field solution provides an excellent description of these data.

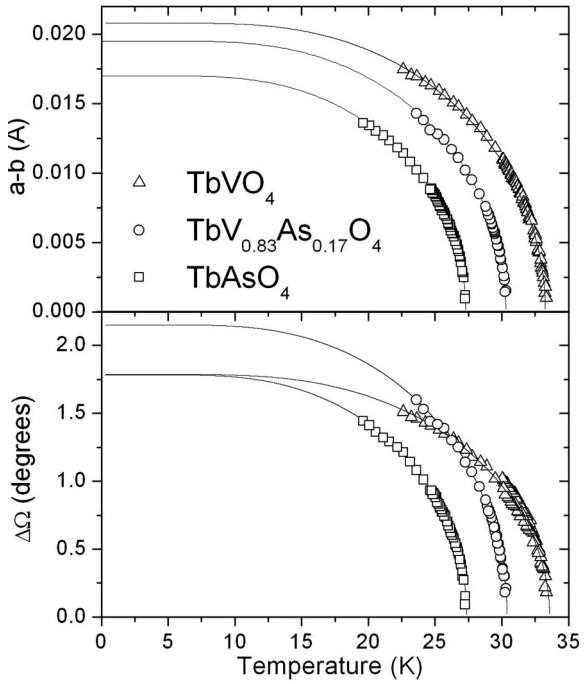

FIG. 3. The top panel shows the measured order parameters, the orthorhombic strains (a-b), in $TbVO_4$, $TbV_{0.83}As_{0.17}O_4$, and $TbAsO_4$. These have been fit to the mean field solution [Eq. (1)] for the order parameter as a function of temperature, which is shown as the solid lines. The lower panel shows the domain orientation Ω splitting of the (12, 0, 0) and (0, 12, 0) Bragg peaks and fits to the same mean field solution. The $TbV_{0.83}As_{0.17}O_4$ Ω splitting was taken as the difference between the majority and minority domains with the strongest Bragg intensity. This was an issue for $TbV_{0.83}As_{0.17}O_4$ alone, as the twinned domains collapsed into a single dominant majority and a minority domain peak within a few degrees of T_C for the pure materials.

Figure 3(b) shows the evolution of the splitting between the twin domain orientation angles Ω that describe the (12, 0, 0) and (0, 12, 0) twin orthorhombic domains below T_C in $TbVO_4$, $TbAsO_4$, and $TbV_{0.83}As_{0.17}O_4$. Again, the temperature dependence of these splittings is very well described by the full mean field solution to the order parameter [Eq. (1)]. This plot follows the evolution of the domain orientation for both the majority and the minority domains present within the field of view of our scattering experiments, for which typical data sets are shown in Fig. 1. For $TbVO_4$ and $TbAsO_4$, a single majority and a minority domain are visible at most temperatures. However, the $TbV_{0.83}As_{0.17}O_4$ data sets are qualitatively different with many domains visible even at temperatures well removed from T_C. For example, the data set for $TbV_{0.83}As_{0.17}O_4$ at $T=26.3$ K (T_C-4 K) shows a total of five twin domains: two majority twin domains at a high scattering angle and three minority twin domains at a low scattering angle. Moreover, the dynamic range in the domain orientation angle spanned by the multiple twin domains is considerably larger than that found in either $TbVO_4$ or $TbAsO_4$ below T_C. Figure 3(b) quantifies this behavior, following the splitting of the majority and minority twin domain orientation angles (Ω) below T_C. The extrapolated, low temperature Ω splitting is very similar for $TbVO_4$ and

$TbAsO_4$ but is considerably larger for $TbV_{0.83}As_{0.17}O_4$, wherein the splitting between the orientation angle Ω of the most intense minority twin and the most intense majority twin domain is plotted.

The order parameter data shown in Fig. 3, along with the fits to full mean field behavior [Eq. (1)], allow a precise determination of the critical temperature T_C in these systems. By fitting both the orthorhombic strain shown in Fig. 3(a) and the twin domain orientation splitting shown in Fig. 3(b), we obtain T_C=33.26(2), 30.32(2), and 27.30(2) K for $TbVO_4$, $TbV_{0.83}As_{0.17}O_4$, and $TbAsO_4$, respectively. In itself, this is a somewhat surprising result, as it shows the T_C for $TbV_{0.83}As_{0.17}O_4$ to lie midway between those of $TbVO_4$ and $TbAsO_4$, despite only 17% of the V ions being replaced by As ions. This is very likely a manifestation of the quenched impurities on the Jahn-Teller driven phase transition in $TbV_{0.83}As_{0.17}O_4$.

The behavior of the twin domains below T_C in $TbV_{0.83}As_{0.17}O_4$ can be qualitatively understood in terms of the pinning of the twin domains by random strains due to the quenched impurities. Clearly, this does not influence the critical properties of the order parameter, the orthorhombic strain, which remains well described by mean field behavior at all temperatures, as is the case for both $TbVO_4$ and $TbAsO_4$. The influence of quenched impurities on twin domain interfaces has been investigated by light scattering techniques,[14] which is expected to be sensitive to such a large scale structure. The present results are qualitatively consistent with these results, showing stable multidomain twin states in $TbV_{0.83}As_{0.17}O_4$, which are distinct from $TbVO_4$ and $TbAsO_4$, and, therefore, a larger volume fraction is taken up by domain interfaces in $TbV_{0.83}As_{0.17}O_4$. However, the change in critical properties previously reported[9] on introduction of quenched impurities is not observed.

IV. MEASUREMENTS OF FLUCTUATIONS OF THE ORTHORHOMBIC STRAIN

A close examination of the scattering data sets at the (12, 0, 0)/(0, 12, 0) Bragg positions in both $TbVO_4$ and $TbAsO_4$ revealed a very interesting longitudinal broadening in the vicinity of T_C. Representative longitudinal scans near the (6, 6, 0) Bragg position in the tetragonal phase and (12, 0, 0) Bragg positions in the orthorhombic phase of $TbVO_4$ are shown in Fig. 4. Very similar data were obtained for $TbAsO_4$, but these are not displayed. Figure 4(a) shows a longitudinal scan through (6, 6, 0) well above T_C at T =47.05 K (T_C+13.8 K), while Fig. 4(d) shows a longitudinal scan through (12, 0, 0) at T=26.75 K, 6.51 K below T_C. Both of these scans have approximately the same intrinsic width, and we consider them to be resolution limited. Figures 4(b) and 4(c), however, show longitudinal scans that are much closer to T_C. Figure 4(b) shows the data just above T_C at T=33.58 K (T_C+0.32 K), while Fig. 4(c) shows the same scan just below T_C at T=32.82 K (T_C−0.44 K). It is clear that both of these longitudinal scans near T_C are appreciably broader than those that are well removed from T_C and, therefore, are not resolution limited.

We associate this broadening with fluctuations in the order parameter, which are similar to that observed near continuous magnetic phase transitions. However, in the present case, fluctuations in the orthorhombic strain lead to a longitudinal broadening of Bragg peaks of the form (6, 6, 0) in the tetragonal phase. Rather than narrowing in angle or reciprocal space as the phase transition is approached, these peaks broaden and decrease in peak intensity as T_C is approached from above. Broadening is also observed below T_C, but the widths of the Bragg peaks quickly fall off, such that all of the scattering in both $TbVO_4$ and $TbAsO_4$ is resolution limited for temperatures more than 2 K below T_C.

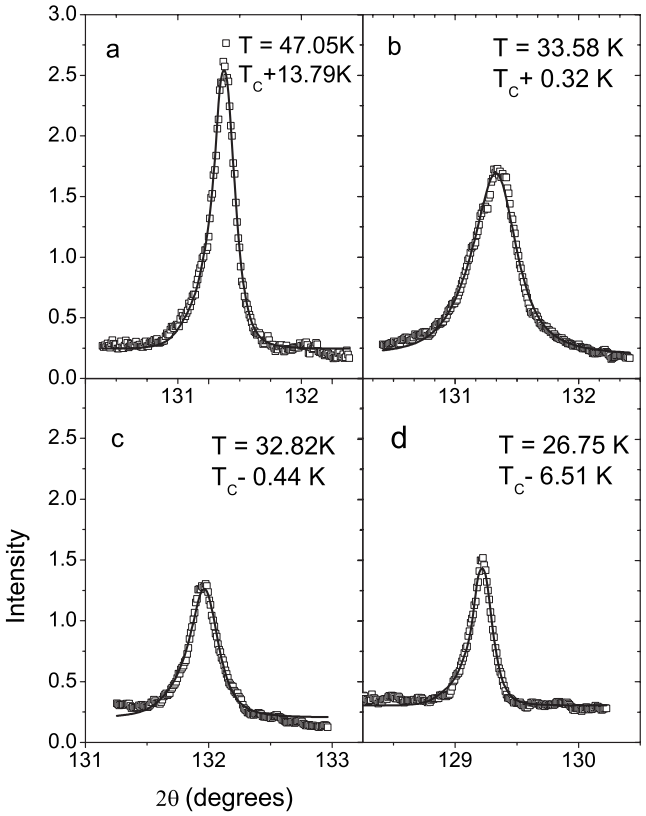

FIG. 4. Representative fits to the longitudinal scans for $TbVO_4$. These data are taken from longitudinal cuts to the full data sets, as shown in Fig. 1(c). (a) and (d) were taken well above and below T_C=33.26(2) K, respectively, and are resolution limited. (b) and (c) are relatively close to T_C and show a substantial broadening in the longitudinal direction. The resolution-corrected longitudinal widths of the profiles were extracted and are plotted as a function of temperature in Figs. 5 and 6.

The data of the form shown in Fig. 4 were fit to an Ornstein–Zernike form,

$$S(2\theta) = \frac{A}{(2\theta - 2\theta_{\text{peak}})^2 + \kappa^2}, \tag{2}$$

which was convoluted with the resolution function appropriate to the measurement. We employed the scattering well above T_C, at $T \sim 50$ K, as the resolution function, assuming that all fluctuation effects are gone at such high temperatures. The results of fitting the $TbVO_4$ data are shown as the solid lines in Fig. 4, and this clearly provides an excellent description of the longitudinal scans at all temperatures. Similar

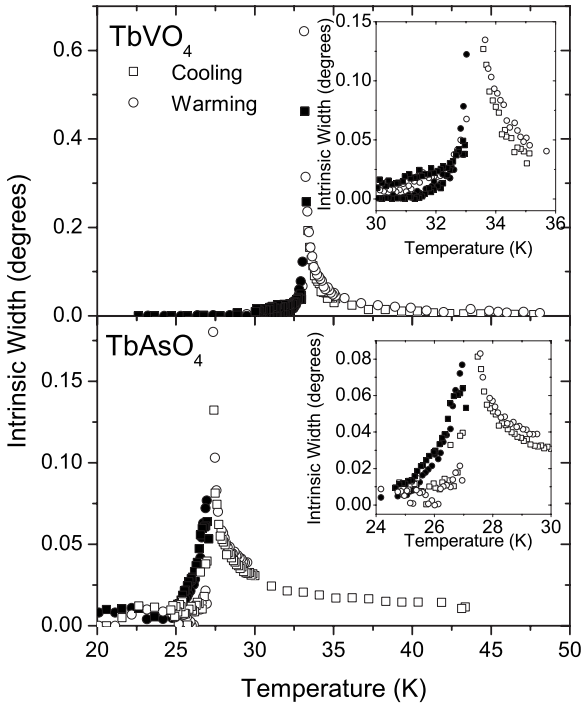

FIG. 5. Resolution-corrected longitudinal widths, or inverse correlation lengths, showing critical fluctuations around the (6, 6, 0) (tetragonal phase) and (12, 0, 0) and (0, 12, 0) (orthorhombic phase) of $TbVO_4$ (top) and $TbAsO_4$ (bottom). Below T_C, the open data points refer to the majority twin domain, while closed data points refer to the minority twin domain. The square and circle data points refer to independent cooling and warming cycles, respectively.

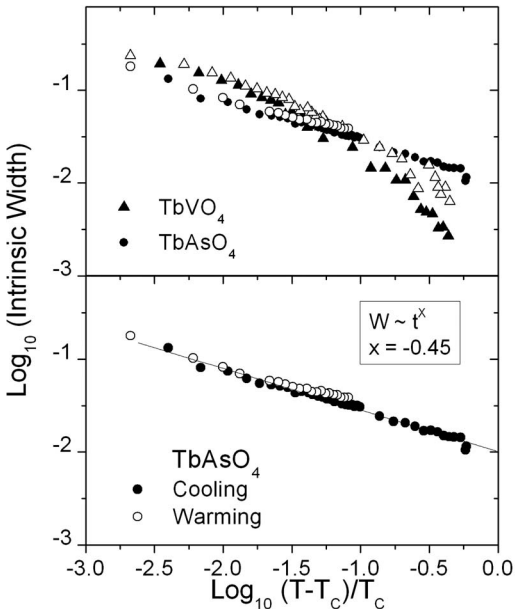

FIG. 6. (Top) The critical behaviors of the longitudinal width κ from Eq. (2), above T_C for $TbVO_4$ and $TbAsO_4$, are shown as a function of reduced temperature. The same data for $TbAsO_4$ along with a fit to a power law divergence characterized by the exponent $x=-0.45\pm0.04$.

quality fits to the $TbAsO_4$ data were also obtained. The resulting intrinsic widths to the longitudinal scans are shown as a function of temperature for $TbVO_4$ in Fig. 5(a) and for $TbAsO_4$ in Fig. 5(b). The data are shown for both independent warming and cooling runs for both materials, although no significant history dependence to the widths of the scattering was observed. For temperatures below T_C, longitudinal scans through both majority and minority twin domains were investigated. Over the narrow range of temperature below T_C for which a finite width can be observed, the intrinsic widths of the majority and minority twin domain peaks differ, with the minority twin peak showing a greater intrinsic width than the majority twin domain, which is consistent with the interpretation of the minority twin domains as being relatively small. A related set of data near T_C was acquired for $TbV_{0.83}As_{0.17}O_4$; however, the relevant longitudinal line shapes were more complicated than those observed in $TbVO_4$ and $TbAsO_4$, and these results are not discussed here.

The most striking and interesting result is that the intrinsic width of the Bragg peaks, which is interpreted as an inverse correlation length, displays a pronounced peak at T_C, which is reminiscent of λ anomalies in the heat capacity of systems undergoing continuous phase transitions. The temperature dependence of the divergence of the intrinsic width, or inverse correlation length, is examined on a log-log plot in Fig. 6, wherein data above T_C in $TbVO_4$ and $TbAsO_4$ are plotted vs reduced temperature $(T-T_C)/T_C$. Again, independent warming and cooling runs are shown, with no history dependence observed. This plot, which employs the same T_C used to describe the critical properties of the order parameter shown in Fig. 3, clearly brings out the power law nature of the divergence of the intrinsic width of the scattering as T_C is approached from above. Figure 6(a) shows these data for both $TbVO_4$ and $TbAsO_4$, and it is clear that both materials display a very similar power law divergence over at least one and half decades in reduced temperature. Figure 6(b) shows the intrinsic width of the longitudinal scan in $TbAsO_4$ alone, wherein a single power law describes its divergence over almost three decades in reduced temperature. The exponent that characterize the divergence is $x=0.45\pm0.04$.

While we have characterized the power law divergence of the inverse correlation length, or intrinsic width, at T_C, we do not have a precise interpretation for this critical phenomenon. In their high-resolution gamma-ray diffraction experiments on $TbVO_4$, Smith and Tanner[7] observed a broadening in the rocking-curve widths, which is the transverse width of the Bragg peaks, as the phase transition was approached from above that somewhat resembles the broadening that we measured. They did not analyze it in detail but suggested that it arose from the strains associated with random internal stresses that relax as the elastic constant C_{66} tends to zero. While such a mechanism could contribute in our case, it is difficult to believe that it would exhibit a critical behavior over such a wide range and with such a well-defined power law behavior as what we have observed.

As previously mentioned, our observed longitudinal broadening of the (6, 6, 0) (tetragonal) and the (12, 0, 0)/(0, 12, 0) (orthorhombic) Bragg peaks in Fig. 5 greatly resembles heat capacity anomalies associated with continuous phase transitions. This may be a natural explanation of the intrinsic width, as the width is inversely proportional to the

fluctuating domain size and, thus, proportional to the volume fraction of the material occupied at any one time by interface. The energy of such a system would scale as the amount of interface, and a longitudinal Bragg peak width scaling as a derivative of the energy, the heat capacity, seems physically reasonable. The critical exponent x may be close to that describing the fluctuation near a mean field, or a mean field tricritical point, for which a large heat capacity exponent characteristic of a divergence is appropriate. At present, we cannot be more precise but hope that the observation and characterization of this critical behavior informs and motivates further work and understanding.

V. COMPARISON TO RELATED STRUCTURAL PHASE TRANSITIONS AND FLUCTUATIONS

We can compare the present results on the order parameter and fluctuations near the Jahn-Teller tetragonal to orthorhombic structural phase transitions in $TbVO_4$, $TbAsO_4$, and $TbV_{0.83}As_{0.17}O_4$ to those in related systems. The principal characteristics of the present results are mean field critical behavior for the orthorhombic strain and the observation of clear fluctuation effects in the vicinity of T_C.

Two topical and well-studied systems that undergo tetragonal to orthorhombic structural phase transitions are the high temperature superconductors $La_{2-x}Ba_xCuO_4$ and $La_{2-x}Sr_xCuO_4$. Critical x-ray and neutron scattering on these materials do not show mean field behavior, but rather the orthorhombic strain goes like the square of the order parameter,[16,17] which is well described by three-dimensional universality. Theoretical expectations for these systems are for a 3D *XY* critical behavior,[18] and this is consistent with what is observed.[16,17] Even qualitatively, it is clear that the growth in the orthorhombic strain with decreasing temperature in $TbVO_4$, $TbAsO_4$, and $TbV_{0.83}As_{0.17}O_4$ is different from that observed in $La_{2-x}Ba_xCuO_4$ and $La_{2-x}Sr_xCuO_4$. When compared to a recent high-resolution x-ray scattering study on the $La_{2-x}Ba_xCuO_4$ system,[17] we can see that the orthorhombic strain grows in a relatively gentle manner with decreasing temperature compared to what is observed in $TbVO_4$, $TbAsO_4$, and $TbV_{0.83}As_{0.17}O_4$. Figure 3 shows that the latter orthorhombic strains grow to approximately half of their saturation values at $0.9T_C$. The same growth in the $La_{2-x}Ba_xCuO_4$ system requires lower temperatures and half of the saturation is only achieved by $\sim 0.7T_C$.

There are differences, of course, between high temperature superconducting copper oxides and the terbium-based oxides that we report here. Cuprates are quasi-two-dimensional, for example, while $TbVO_4$, $TbAsO_4$, and $TbV_{0.83}As_{0.17}O_4$ are three dimensional. Most notably, however, the magnetic Cu^{2+} ion in $La_{2-x}Ba_xCuO_4$ and $La_{2-x}Sr_xCuO_4$ is not Jahn-Teller active—a single hole resides in a nondegenerate d orbital. This would appear to be the most likely source for the difference in critical behaviors. $TbVO_4$, $TbAsO_4$, and $TbV_{0.83}As_{0.17}O_4$ possess Tb^{3+} ions whose orbitals and the occupation of the orbitals change on going through T_C, likely generating long range strain fields with concomitant mean field behavior.

Another interesting comparison is to other Tb^{3+}-based transition metal oxides. Here, an interesting comparison can be made to a very recent high-resolution x-ray scattering study of the cubic pyrochlore $Tb_2Ti_2O_7$.[19] This geometrically frustrated magnetic material does not undergo a structural phase transition at a finite temperature, but recent x-ray scattering measurements observe a broadening of the allowed structural Bragg peaks at low temperatures. These have been interpreted as fluctuations above a very low temperature Jahn-Teller phase transition, which is either never realized or realized at only unattainably low temperatures. Indeed, to our knowledge, the present work is the only other study of structural phase transitions that show such a critical broadening of the Bragg peaks in the vicinity of T_C. The temperature scale over which these fluctuations are observed is quite different in $Tb_2Ti_2O_7$ as compared to those in $TbVO_4$, $TbAsO_4$, and $TbV_{0.83}As_{0.17}O_4$. In the present case, the broadening of the Bragg peaks appears as a critical phenomenon and the strongest fluctuation effects fall off within a few degrees of T_C. In contrast, the Jahn-Teller-type fluctuations in $Tb_2Ti_2O_7$ occur coincident with the formation of a spin liquid state and are measurable over an extended regime of temperature from 20 to 0.3 K.

Finally, we return to the issue of mean field criticality vs the criticality associated with random fields. We did not observe a departure from the mean field criticality associated with the random fields in $TbV_{0.83}As_{0.17}O_4$. This may be because the random fields associated with the disorder are too weak to influence the critical behavior in the range of reduced temperatures that we could access. A measure of the strength of the disorder and associated random fields is the extent to which they depress the transition temperature. The observed T_C for our mixed sample was 30.32 K, lower than the value of 32.25 K as expected from a linear variation in T_C between the two end members. This depression in T_C confirms that disorder is relevant and that the associated random fields are present. In some related systems that have been studied, such as $DyAs_xV_{1-x}O_4$ (Refs. 20 and 21) and $KH_2As_xP_{1-x}O_4$,[22] however, as well as in dilute antiferromagnetic systems,[11] the depressions in T_C were larger and a random-field critical behavior was clearly observed.

VI. CONCLUSIONS

We have studied the critical properties near the Jahn-Teller tetragonal to orthorhombic structural phase transitions in $TbVO_4$, $TbAsO_4$, and $TbV_{0.83}As_{0.17}O_4$ by using high-resolution x-ray scattering. These results show that the order parameter, the orthorhombic strain, exhibits mean field criticality in all three materials. The disordered member of this series, $TbV_{0.83}As_{0.17}O_4$, is distinguished only in so far that it exhibits a wide dynamic range of majority and minority orthorhombic twin domain orientations, and these are stable to low temperatures. We ascribe this to the pinning of the domain structure by random strains arising from the quenched disorder in $TbV_{0.83}As_{0.17}O_4$.

We also observe very interesting fluctuation effects in $TbVO_4$ and $TbAsO_4$ in the vicinity of T_C. These are manifested in a longitudinal broadening of the (6, 6, 0) Bragg peaks in the tetragonal phase, which split to become the (12, 0, 0) and (0, 12, 0) Bragg peaks in the orthorhombic low temperature phase. This broadening exhibits a power law divergence at T_C, in $TbVO_4$ and $TbAsO_4$, with a critical exponent $x=0.45\pm0.04$. We hope that this latter work informs and motivates a full theoretical understanding of these fluctuation phenomena.

ACKNOWLEDGMENT

This work was supported by NSERC.

[1] M. T. Hutchings, R. Scherm, S. H. Smith, and S. R. P. Smith, J. Phys. C **8**, L393 (1975).
[2] R. J. Elliot, R. T. Harley, W. Hayes, and S. R. P. Smith, Proc. R. Soc. London, Ser. A **328**, 217 (1972).
[3] G. A. Gehring and K. A. Gehring, Rep. Prog. Phys. **38**, 1 (1975).
[4] W. Schäfer and G. Will, Acta Crystallogr., Sect. B: Struct. Crystallogr. Cryst. Chem. **35**, 588 (1979).
[5] R. T. Harley and R. M. Macfarlane, J. Phys. C **8**, L451 (1975).
[6] G. Will, H. Gobel, C. F. Sampson, and J. B. Forsyth, Phys. Lett. **38A**, 207 (1972).
[7] S. R. P. Smith and B. K. Tanner, J. Phys. C **11**, L717 (1978).
[8] Y. Hirano, N. Wakabayashi, C.-K. Loong, and L. A. Boatner, Phys. Rev. B **67**, 014423 (2003).
[9] C.-H. Choo, H. P. Schriemer, and D. R. Taylor, Phys. Rev. B **61**, 11197 (2000).
[10] Y. Imry and S. K. Ma, Phys. Rev. Lett. **35**, 1399 (1975).
[11] D. P. Belanger, in *Spin Glasses and Random Fields*, edited by A. P. Young (World Scientific, Singapore, 1998), p. 251.
[12] G. Jasiolek and H. A. Dabkowska, J. Cryst. Growth **79**, 534 (1986).
[13] P. Hagenmuller, J. Less-Common Met. **110**, 225 (1985).
[14] H. P. Schriemer, C.-H. Choo, and D. R. Taylor, Phys. Rev. B **59**, 8351 (1999).
[15] W. Berkhahn, H. G. Kahle, L. Klein, and H. C. Schopper, Phys. Status Solidi B **55**, 265 (1973).
[16] D. Vaknin, S. K. Sinha, D. E. Moncton, D. C. Johnston, J. M. Newsam, C. R. Safinya, and H. E. King, Jr., Phys. Rev. Lett. **58**, 2802 (1987); R. J. Birgeneau, C. Y. Chen, D. R. Gabbe, H. P. Jenssen, M. A. Kastner, C. J. Peters, P. J. Picone, Tineke Thio, T. R. Thurston, H. L. Tuller, J. D. Axe, P. Boni, and G. Shirane, *ibid.* **59**, 1329 (1987); P. Boni, J. D. Axe, G. Shirane, R. J. Birgeneau, D. R. Gabbe, H. P. Jenssen, M. A. Kastner, C. J. Peters, P. J. Picone, and T. R. Thurston, Phys. Rev. B **38**, 185 (1988); T. R. Thurston, R. J. Birgeneau, D. R. Gabbe, H. P. Jenssen, M. A. Kastner, P. J. Picone, N. W. Preyer, J. D. Axe, P. Boni, G. Shirane, M. Sato, K. Fukuda, and S. Shamoto, *ibid.* **39**, 4327 (1989).
[17] Y. Zhao, B. D. Gaulin, J. P. Castellan, J. P. C. Ruff, S. R. Dunsiger, G. D. Gu, and H. A. Dabkowska, Phys. Rev. B **76**, 184121 (2007).
[18] J. C. Le Guillou and J. Zinn-Justin, Phys. Rev. Lett. **39**, 95 (1977); J. C. Le Guillou and J. Zinn-Justin, Phys. Rev. B **21**, 3976 (1980).
[19] J. P. C. Ruff, B. D. Gaulin, J. P. Castellan, K. C. Rule, J. P. Clancy, J. Rodriguez, and H. A. Dabkowska, Phys. Rev. Lett. **99**, 237202 (2007).
[20] J. T. Graham, J. H. Page, and D. R. Taylor, Phys. Rev. B **44**, 4127 (1991).
[21] K. A. Reza and D. R. Taylor, Phys. Rev. B **46**, 11425 (1992).
[22] D. R. Taylor, J. T. Love, G. J. Topping, and J. G. A. Dane, Phys. Rev. B **72**, 052109 (2005).